

## Strong magnetoelectric coupling in Tb–Fe/Pb(Zr<sub>0.52</sub>Ti<sub>0.48</sub>)O<sub>3</sub> thin-film heterostructure prepared by low energy cluster beam deposition

Shifeng Zhao, Yujie Wu, Jian-guo Wan,<sup>a)</sup> XinWei Dong,  
Jun-ming Liu, and Guanghou Wang

National Laboratory of Solid State Microstructures and Department of Physics, Nanjing University,  
Nanjing 210093, People's Republic of China,  
and International Center for Materials Physics, Chinese Academy of Sciences, Shenyang 110016, China

(Received 30 November 2007; accepted 11 December 2007; published online 10 January 2008)

The magnetoelectric Tb–Fe/Pb(Zr<sub>0.52</sub>Ti<sub>0.48</sub>)O<sub>3</sub> thin-film heterostructure was prepared by low energy cluster beam deposition. The microstructures, ferroelectric property, leakage current, and magnetization, as well as magnetoelectric effect were investigated for the heterostructure. It is shown that the thin-film heterostructure displays the well-defined microstructure with clear interface. The heterostructure not only exhibits good ferromagnetic and ferroelectric properties, but also possesses strong magnetoelectric effect. The present work provides an ideal avenue to prepare magnetoelectric composite films and facilitates their applications on the microelectromechanical system devices. © 2008 American Institute of Physics. [DOI: 10.1063/1.2831695]

In recent years, magnetoelectric films have drawn a continually increasing interest due to their potential applications in the microelectromechanical system (MEMS) devices.<sup>1</sup> By growing composite films combined with piezoelectric and magnetostrictive materials, the strong magnetoelectric coupling effect could be achieved due to product property. So far, much work has been done to prepare the composite films by combining perovskite ferroelectric oxides [e.g., Pb(Zr<sub>0.52</sub>Ti<sub>0.48</sub>)O<sub>3</sub> (PZT), BaTiO<sub>3</sub>] with ferromagnetic oxides (e.g., CoFe<sub>2</sub>O<sub>4</sub>, La<sub>0.67</sub>Sr<sub>0.33</sub>MnO<sub>3</sub>).<sup>2–5</sup> Due to low magnetostriction of the ferromagnetic oxides, the reported magnetoelectric effects in these all-oxide composite films are generally not strong.

It is well known that *R* (rare earth)-Fe iron alloy possesses giant magnetostriction, being an order of magnitude greater than the ferromagnetic oxides.<sup>6</sup> The previous investigations have shown that the magnetoelectric effect in the bulk laminate consisted of *R*-Fe alloy and ferroelectric oxide is much larger than that of the all-oxide laminates.<sup>7–9</sup> Therefore, for the laminated composite thin film (i.e., thin-film heterostructure), it could be expected that magnetoelectric effect would be enhanced significantly if *R*-Fe alloy is used in the magnetostriction layer. However, by conventional film preparation means, since the phase-formation temperature of *R*-Fe alloy is very high (the substrate is generally heated above 500 °C), it is unavoidable to bring about serious oxygen diffusion from PZT oxide to *R*-Fe alloy. As a result, both magnetostriction in *R*-Fe alloy and piezoelectricity in PZT are seriously suppressed. Moreover, the serious oxygen diffusion would also generate a new interface layer, which further significantly decreases the magnetoelectric coupling efficiency.<sup>8</sup> Due to these factors, so far, few investigations on relative work have been carried out.

Recently, we have developed an effective preparation method, namely, low energy cluster beam deposition (LECBD), to prepare the nanostructured Tb–Fe film,<sup>10</sup> which makes it possible to prepare the well-defined microstructured

thin-film heterostructure consisted of *R*-Fe alloy and ferroelectric oxide. We have demonstrated that such nanostructured Tb–Fe film possesses higher magnetostriction than the common Tb–Fe films prepared by other methods.<sup>10</sup> More importantly, during LE CBD process, the phase formation of Tb–Fe nanoclusters (or nanoparticles) is achieved in the condensation chamber with high temperature, while the deposition of Tb–Fe nanocluster beam onto the substrate is achieved in another high vacuum chamber with low energy and low temperature (e.g., room temperature). Both processes are completely independent of each other. Therefore, even if the substrate is ferroelectric oxide, the degree of the interfacial reaction or diffusion between Tb–Fe alloy and ferroelectric oxide would be greatly suppressed. In this letter, we report the preparation of Tb–Fe/PZT bilayer thin-film heterostructure by LE CBD process. The well-defined microstructured with clear interface is achieved in the heterostructure, and strong magnetoelectric effect is observed.

A 100 nm thick PZT film deposited on the Pt/Ti/SiO<sub>2</sub>/Si wafer was used as the substrate in this work. The details on the preparation of PZT thin film could be found elsewhere.<sup>11</sup> The substrate was blocked by a mask with the open holes of 0.2 mm in diameter. A dc-magnetron-sputtering-gas-aggregation cluster source was used to produce the cluster beam and a 5 cm diameter TbFe<sub>2</sub> alloy plate was used as the sputtering target. Both argon and helium gases were used as the condensed inert carrier gases for the nanoclusters. After passing through the skimmer, a high-orient Tb–Fe nanocluster beam forms. The Tb–Fe nanocluster beam finally deposits onto the surface of the PZT film through the open holes of the mask. During LE CBD process, the background pressure of the system was  $4 \times 10^{-5}$  Pa. The final thickness of the Tb–Fe layer was  $\sim 300$  nm. The details on LE CBD process could be found elsewhere.<sup>10</sup> After deposition, not taking off the mask, a Pt electrode layer was deposited on the Tb–Fe dots via pulse laser deposition. The structure of the thin-film heterostructure is sketched in inset (a) of Fig. 1.

Figure 1 shows the surface scanning electron microscopy (SEM) image of the Tb–Fe layer in the heterostructure.

<sup>a)</sup> Author to whom correspondence should be addressed. Electronic mail: wanjg@nju.edu.cn.

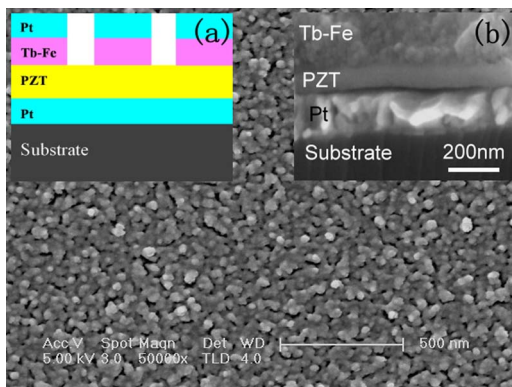


FIG. 1. (Color online) The surface SEM image of the Tb–Fe layer in the thin-film heterostructure. Inset (a) is a sketch of the heterostructure and inset (b) is the fractured cross-sectional SEM image of the heterostructure.

It is seen that the Tb–Fe layer is compactly assembled by the regular spherical nanoparticles with average diameter of  $\sim 30$  nm, which are distributed uniformly and adjacent with each other. Inset (b) of Fig. 1 shows the cross-sectional SEM image of the thin-film heterostructure. One observes that the interface between Tb–Fe and PZT layers is clear and no transition layer is observed. In addition, the x-ray diffraction result (not shown here) also proved that there existed no additional phase peaks except PZT and Tb–Fe phase peaks.

The vertical-transport resistivity measurement for the heterostructure yields a resistivity of  $\sim 2.1 \times 10^{10} \Omega \text{ cm}$  at zero bias, indicating that the heterostructure is a very good dielectric insulator. Figure 2(a) presents the polarization versus electric field ( $P$ - $E$ ) hysteresis loops for the heterostructure measured by a RT66 ferroelectric testing unit with the

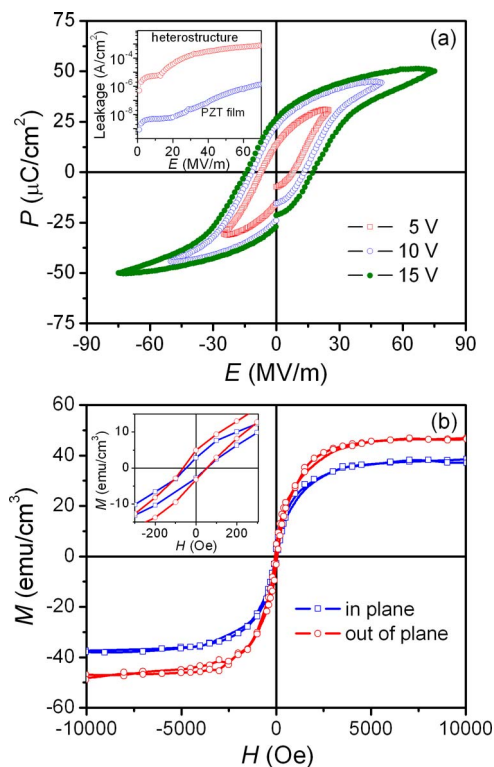


FIG. 2. (Color online) (a) Polarization vs electric field hysteresis ( $P$ - $E$ ) loops for the thin-film heterostructure. Inset is the variation of leakage current density with the applied electric field. (b) The field dependent magnetization ( $M$ - $H$ ) curves for the thin-film heterostructure.

applied electric voltage of 5–15 V. The well-defined ferroelectric loops are observed. Under the applied electric voltage of 15 V, the saturation polarization and remanent polarization are  $P_s = 51 \mu\text{C}/\text{cm}^2$  and  $P_r = 27 \mu\text{C}/\text{cm}^2$ , respectively, both of which only have a very slight decrease compared with the pure PZT film ( $P_s = 58 \mu\text{C}/\text{cm}^2$  and  $P_r = 34 \mu\text{C}/\text{cm}^2$ ). Such slight decrease in ferroelectric properties of the heterostructure should be attributed to the increase of oxygen vacancy concentration in PZT layer, which brings about difficulty for the mobility of domain walls in a certain degree and further leads to the decrease in polarization.<sup>12</sup>

In order to further understand this, we performed the leakage current density measurement at room temperature, as shown in inset of Fig. 2(a). It is clearly shown that the leakage current density in the heterostructure is quite low, e.g., only being  $\sim 1.5 \times 10^{-4} \text{ A}/\text{cm}^2$  even under the higher electric field of 30 MV/m. In spite of this, we found that the leakage current density in the heterostructure was still higher than that of the pure PZT film, which indicates the increase of free carrier density in PZT layer of the heterostructure.<sup>13</sup> It was reported that, under high electric field, the leakage current in the ferroelectric film was closely relative to the oxygen vacancies, which could be well explained by a conduction mechanism based on Schottky emission model.<sup>14</sup> Accordingly, we infer that there should appear induced oxygen vacancies in PZT layer near the interface during preparation of the heterostructure, which obviously originates from the slight oxygen diffusion from PZT layer to Tb–Fe layer. In fact, though the LECBD process is under the low energy, the Tb–Fe nanoclusters still possess certain energy (in the range of 0.01–0.1 eV/atom). Due to the very strong oxidation activity for the rare-earth Tb–Fe alloy, some Tb–Fe nanoclusters with higher energy may have a chance to take oxygen from PZT layer when they land onto the PZT substrate, consequently, giving rise to the introduction of oxygen vacancies.

Figure 2(b) presents the field dependent magnetization ( $M$ - $H$ ) curves for the heterostructure measured by a superconducting quantum interference device. The heterostructure exhibits the well-defined magnetic hysteresis loops. One observes that both in-plane and out-of-plane coercive fields are the same as only  $H_c \sim 60 \text{ Oe}$ , much lower than that of the bulk Tb–Fe alloy, while the in-plane and out-of-plane saturation magnetizations are  $\sim 38$  and  $\sim 47 \text{ emu}/\text{cm}^3$ , respectively. According to our previous work,<sup>10</sup> the Tb–Fe nanostructured film prepared by LECBD process exhibits high magnetostriction under the low magnetic field, e.g., typically being  $\lambda \sim 300 \times 10^{-6}$  under dc magnetic bias  $H_{\text{bias}} = 3.5 \text{ kOe}$ . Since magnetoelectric effect in a two-phase composite mainly originates from the interfacial stress transfer between the magnetostrictive and the ferroelectric phases, such low coercivity and high magnetostriction are significantly beneficial to the magnetoelectric coupling.<sup>11,15</sup>

We subsequently measured the magnetoelectric effect for the heterostructure. Both  $H_{\text{bias}}$  and small ac magnetic field (10 Oe) were applied along the film plane. The induced voltage increment  $|\Delta V_{\text{ME}}|$  was recorded by a lock-in amplifier (SRS Inc., SR830). Figure 3 plots the  $H_{\text{bias}}$  dependence of  $|\Delta V_{\text{ME}}|$  at a given ac magnetic field frequency  $f = 1.0 \text{ kHz}$ . One observes that the film exhibits strong magnetoelectric coupling. With increasing  $H_{\text{bias}}$ , the  $|\Delta V_{\text{ME}}|$  value rapidly increases, reaching the maximum value of  $14 \mu\text{V}$  at  $H_{\text{bias}}$

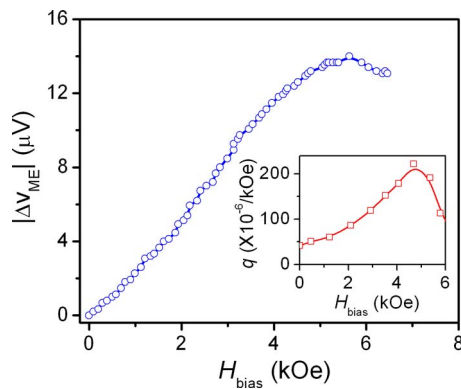


FIG. 3. (Color online) The  $H_{\text{bias}}$  dependence of the induced magnetoelectric voltage increment  $|\Delta V_{\text{ME}}|$  at a given dc magnetic frequency  $f=1.0$  kHz for the thin-film heterostructure. Inset is the  $H_{\text{bias}}$  dependence of piezomagnetic coefficient  $q$  for the pure Tb-Fe nanostructured film prepared by LECBD process.

$=5.5$  kOe, and then drops slowly. The calculated maximum increment of the magnetoelectric voltage coefficient is as high as  $\sim 140$  mV/cm Oe, larger than that of the reported all-oxide ferroelectric-ferromagnetic composite film.<sup>2-4</sup> Inset of Fig. 3 further plots the  $H_{\text{bias}}$  dependence of piezomagnetic coefficient  $q$  ( $=\delta\lambda/\delta H_{\text{bias}}$ ) for the pure Tb-Fe nanostructured film prepared by LECBD process. Compared with these two curves, we find that both  $|\Delta V_{\text{ME}}|$  in heterostructure and  $q$  in Tb-Fe film have the similar change trend with  $H_{\text{bias}}$ . This indicates that the magnetoelectric coupling in the heterostructure should be dominated by the magnetic-mechanical-electric transform through the stress-mediated transfer, which is well in agreement with the model proposed by Srinivasan *et al.*<sup>16</sup> In addition, we believe that the magnetoelectric effect in the heterostructure could be further enhanced by controlling the oxygen diffusion in the interface, which could be achieved if the kinetic energy of the nanocluster beam is modulated appropriately. The relative investigations are now underway.

In summary, the Tb-Fe/PZT thin-film heterostructure was prepared by LECBD process. The heterostructure shows a well-defined microstructure with clear interface. The slight

oxygen diffusion between PZT and Tb-Fe layers was testified by the leakage current density measurement. In spite of this, the heterostructure exhibits good ferroelectric and ferromagnetic properties, and the strong magnetoelectric effect was observed in the heterostructure. The present work opens an ideal avenue to prepare the magnetoelectric composite films, which facilitates their applications on MEMS devices.

This work was financially supported by the National Natural Science Foundation of China (Grant Nos. 10774070, 90406024, and 90606002), the Provincial Nature Science Foundation of Jiangsu in China (BK2006123), the National Key Projects for Basic Research of China (2002CB613303 and 2006CB921802), and the Program for New Century Excellent Talents in University of China (NCET-07-0422).

- <sup>1</sup>N. A. Spaldin and M. Fiebig, *Science* **309**, 391 (2005).
- <sup>2</sup>Y. G. Ma, W. N. Cheng, M. Ning, and C. K. Ong, *Appl. Phys. Lett.* **90**, 152911 (2007).
- <sup>3</sup>J. P. Zhou, H. C. He, Z. Shi, and C. W. Nan, *Appl. Phys. Lett.* **88**, 013111 (2006).
- <sup>4</sup>H. Zheng, J. Wang, L. Mohaddes-Ardabili, M. Wuttig, L. Salamanca-Riba, D. G. Schlom, and R. Ramesh, *Appl. Phys. Lett.* **85**, 2035 (2004).
- <sup>5</sup>W. Eerenstein, M. Wiora, J. L. Prieto, J. F. Scott, and N. D. Mathur, *Nat. Mater.* **6**, 348 (2007).
- <sup>6</sup>R. C. O'handley, *Modern Magnetic Materials: Principles and Applications* (Wiley, New York, 2000).
- <sup>7</sup>J. Ryu, A. V. Carazo, K. Uchino, and H. E. Kim, *Jpn. J. Appl. Phys., Part 1* **40**, 4948 (2001).
- <sup>8</sup>C. W. Nan, G. Liu, and Y. H. Lin, *Appl. Phys. Lett.* **83**, 4366 (2003).
- <sup>9</sup>G. Srinivasan, A. A. Bush, K. E. Kamentsev, V. F. Meshcheryakov, and Y. K. Fetisov, *Appl. Phys. A: Mater. Sci. Process.* **78**, 721 (2004).
- <sup>10</sup>S. F. Zhao, F. Bi, J. G. Wan, M. Han, F. Q. Song, J. M. Liu, and G. H. Wang, *Nanotechnology* **18**, 265705 (2007).
- <sup>11</sup>J. G. Wan, X. W. Wang, Y. J. Wu, M. Zeng, Y. Wang, H. Jiang, W. Q. Zhou, G. H. Wang, and J. M. Liu, *Appl. Phys. Lett.* **86**, 122501 (2005).
- <sup>12</sup>J. F. Scott and M. Dawber, *Appl. Phys. Lett.* **76**, 3801 (2000).
- <sup>13</sup>C. Wang, M. Takahashi, H. Fujino, X. Zhao, E. Kume, T. Horiuchi, and S. Sakai, *J. Appl. Phys.* **99**, 054104 (2006).
- <sup>14</sup>K. Numata, *Thin Solid Films* **515**, 2635 (2006).
- <sup>15</sup>T. Wu, M. A. Zurbuchen, S. Saha, R.-V. Wang, S. K. Streiffer, and J. F. Mitchell, *Phys. Rev. B* **73**, 134416 (2006).
- <sup>16</sup>G. Srinivasan, E. T. Rasmussen, J. Gallegos, R. Srinivasan, Yu. I. Bokhan, and V. M. Laletin, *Phys. Rev. B* **64**, 214408 (2001).